CSTAM 2012-B03-0007

Delaying transition further with the aid of a short compliant panel in a Blasius boundary layer flow

I. Bori，K.S. Yeo，H-S. Dou，X. Zhao

National University of Singapore

Zhejiang Sci-Tech University

第七届全国流体力学学术会议

2012 年 11 月 12—14 日 广西·桂林

DELAYING TRANSITION FURTHER WITH THE AID OF A SHORT COMPLIANT PANEL IN A BLASIUS BOUNDARY LAYER FLOW[1]

I. Bori*，K.S. Yeo*，H-S. Dou+，[2]，X. Zhao*
* Fluid Mechanics Division,
Department of Mechanical Engineering, National University of Singapore, Singapore 117576
+ Faculty of Mechanical Engineering & Automation,
Zhejiang Sci-Tech University, Hangzhou 310018, China

Abstract: The cost of fuelling especially for those in the transport industries could be reduced drastically if there is a means of reducing drag force over their vehicles while in motion. One way to overcome this is to use compliant (membrane) surface; a passive control means which has been proved in various theoretical studies as a promising tool in delaying transition further. In this paper, following the earlier work done on flow over rigid wall within a Blasius boundary layer, we account for the current study carried out on the evolution of pulse-initiated disturbance wavepackets over a finite-length compliant panel by direct numerical simulation (DNS) method. For the single-panel case, a finite section of the wall from $X = x/\delta_0 =$ 450 -762, was replaced by a tensioned membrane on a viscoelastic foundation, whose properties were designed to inhibit the development of compliant-wall modes. Where δ_0 is the displacement thickness at the perturbation location. A small amplitude vertical initiating delta pulse was introduced from the wall streamwise location $X_0 = 349.4$ ($x_0 = 81$cm), and study in detail both spatially and spectrally how the wavepackets generated evolve from the initiating point to the breakdown location over a Blasius boundary layer. The simulation results showed that, the upstream intervention by the finite compliant panel effectively delayed the onset of the incipient turbulent spot by a further distance of $\Delta x = 550$, when compared with the rigid wall case results that earlier broke down at $X = 1420$. This represents an approximately 51% increase in the transition distance measured from the point of wavepacket initiation. Spectral study indicated that the relatively short compliant panel was able to effectively weaken the primary 2-D Tollmien-Schlichting (TS) wave mode, thereby extending the linear regime, so that resultant wavepacket after the panel is dominated by two oblique wave modes and this is the effective strategy of transition delay.

Keywords compliant, boundary layer, wavepackets

Introduction

Boundary layer transition has been an interesting topic to many researchers since some decades ago, because the state of the boundary layer, whether laminar or turbulent, has a direct effect for example on the drag force and heat transfer performance of many engineering devices. In the real life situation, laminar state cannot be sustained for over a long period of time before turbulent state quickly set in, which is usually associated with much drag force. Using compliant (membrane) panel which is one of the passive control means has been proved successfully in

1）基金资助项目
2）Email：huashudou@yahoo.com

many theoretical studies as a possible way of delaying transition further in a boundary layer. Advantages of using compliant panel in delaying transition further includes: (i) does not require any sophisticated control equipment or feedback system, and (ii) also less expensive to implement compare with the active control type. Studies on the effect of complaint walls on flow stability were inspired by Kramer (1957, 1960)'s observation of swimming dolphins in the late 1950s. Kramer assumed that their high propulsive efficiency should be ascribed to the compliance of their skin. He then carried out experiments in water by dragging a torpedo covered with a complaint device conceived to mimic the dolphin's skin and achieved drag reduction of more than 50 % compared to that of the rigid wall case.

After this pioneer observation by Kramer, other researchers who had conducted experiments in this area include: Puryear (1962), Nisewanger (1964), Ritter & Porteous (1965), Fisher & Blick (1966), Blick & Walters (1968), Chu & Blick (1969). Bushnell et al. (1977) gave a review of complaint wall drag reduction research up till the mid-1970. They also discussed the potential of compliant surfaces for turbulent drag reduction. Gaster (1987) tested samples of compliant layers in a large towing tank and concluded that viscoelastic compliant layers with the appropriate properties are able to reduce the growth of the TS waves over the corresponding rigid surfaces provided that unstable fluid-surface interaction modes could be avoided or held in check. Willis (1986) and Gaster (1987) further showed that some compliant surfaces could reduce the growth of TS waves by an order of magnitude if wall parameters, such as stiffness and damping are optimally tuned or balanced. Subsequent works include Lee et al. (1995), Colley et al. (1999) and Huang et al. (2007).

While in the numerical investigation realm, a series of methods have been developed for investigating boundary-layer instability, transition and transition control. These methods include: Turbulence Modeling (TM), Large Eddy Simulation (LES), Linear Stability Theory (LST), Parabolized Stability Equation (PSE) and Direct Numerical Simulation (DNS). This reported work is about DNS, and the probably first temporal direct numerical simulation of boundary-layer waves over a complaint surface (tensioned membrane to be specific) was performed by Domaradzki & Metacalfe (1987). They studied the temporal and spatial behavior of the terms in the kinetic energy balance equation and verified the class A and class B character of the computed waves. Hall (1988) also developed a temporal simulation algorithm for simulating 2D instability waves over soft polyvinyl chloride (PVC) layers. Metcalfe et al. (1991) reported their 3D temporal DNS work on boundary layer flow instability over a compliant panel. Their simulation showed that nonlinear secondary instabilities could arise and cause the flow to become unstable when it was predicted to be stable by linear theory. Davies & Carpenter (1997)'s simulation of boundary-layer stability over finite compliant panel was perhaps the first work done on the linear Navier-Stokes simulations of flow stability over a compliant surface. A novel vorticity-velocity method was used in their simulations. The main conclusion drawn by Davies and Carpenter from their simulations is that panels as short as one TS wavelength remain effective at suppressing TS waves. They also demonstrated that certain very short compliant panels are even more effective at wave suppression than longer ones with the same properties.

Wiplier & Ehrenstein (2000, 2001) adopted the primitive-variable method to simulate the spatial evolution of 2D disturbances in a boundary-layer flow over compliant membranes and panels. Their simulation results re-affirmed the validity of the linear stability theory and show that absolute instability could arise from the coalescence between an upstream propagating evanescent

mode and downstream propagating TS wave as was suggested by Yeo et al. (1999). Wang et al. (2001) employed a 2-D vorticity-streamfunction method for spatially simulating the unsteady waves over finite-length membranes. Two cases with different tensions were investigated in some details. Also, Wang (2003), Wang et al. (2005) and Zhao (2006) conducted spatial direct numerical simulation of two-dimensional and three-dimensional transitional boundary layer flows over finite compliant surfaces. They concluded that compliant coatings with selected properties are able to reduce the growth rates of linear TS waves and three-dimensional subharmonic nonlinear instabilities, but may not be effective against three-dimensional fundamental nonlinear instabilities. Later works include Davies (2005), Zhao (2006).

From the literature so far, no detailed work had been reported on the spatial evolution and spectral analysis of wavepacket which was generated through a delta (vertical v-velocity component) pulse disturbance upstream of the flow, and allowed the disturbance to propagate over a compliant panel within a Blasius boundary layer. The main motives behind this study are (i) to investigate if by replacing a small section of the computational rigid wall with a finite length of compliant panel could delay transition further, thereby resulting in drag reduction and (ii) to see clearly if the membrane panel actually suppress the 2-D TS waves or not from the spectrum analysis point of view.

1 Numerical Simulation

1.1 Numerical scheme

Same direct numerical simulation (DNS) code which was modified by Zhao (2006) for the simulations of wavepacket over the compliant panels in a Blasius boundary layer was used for the incompressible Navier-Stokes equations:

$$\frac{\partial u_i}{\partial x_i} = 0 \qquad (1.1)$$

$$\frac{\partial u_k}{\partial t} + \frac{\partial}{\partial x_i}\left(c_2\bar{u}_i u_k + c_2 u_i \bar{u}_k + c_1 u_i u_k\right) = \frac{\partial}{\partial x_i}\left(\frac{1}{\mathrm{Re}}\frac{\partial u_k}{\partial x_i}\right) - \frac{\partial p}{\partial x_k} \qquad (1.2)$$

where i, j, k = 1, 2, 3 represent the streamwise (x), the wall normal (y) and spanwise (z) coordinates of the Cartesian frame respectively. The perturbation form of the Navier-Stokes equations (1.1) and (1.2) is obtained by letting **Error! Reference source not found.** $c_1 = c_2 = 1.0$, and **Error! Reference source not found.** $\bar{u}_i$ represent the components of the base flow, where the base flow used in the present study is the non-parallel Blasius boundary layer profile. The numerical schemes and their associated discretization methods had already been described in detail by Yeo et al (2010). The Reynolds number Re is based on the free-stream velocity U_∞ .The tensioned membrane (compliant panel) displacement is governed by:

$$m\frac{\partial^2 \eta}{\partial t^2} - T\left(\frac{\partial^2 \eta}{\partial x^2} + \frac{\partial^2 \eta}{\partial z^2}\right) + d\frac{\partial \eta}{\partial t} + k\eta = -p_w \qquad (1.3)$$

where η represents the normal or y-displacement of the membrane surface. T represents the surface tension, m the mass per unit area of membrane, d is the damping coefficient, and k is the equivalent foundation elastic constant, and **Error! Reference source not found.** as the external pressure acting on the membrane surface. As for the numerical methods aspects, Wang et al (2005) already gave more details about this. The iterative fractional time step method used for the rigid wall case was extended to include fluid-structure interaction. The temporal and spatial terms of the tensioned membrane of equation (1.3) were discretized by the second-order backward-Euler scheme and fourth-order accurate central-difference scheme respectively. At each time step, the flow variables and wall displacement were iterated to convergence.

1.2 Simulation process and computational grid

Computational domain used for the simulation spans $310 \le X \le 1510$ in the streamwise (X) direction,**Error! Reference source not found.** $0 \le Y \le 54$ in the wall normal (Y) direction and **Error! Reference source not found.** $-172 \le Z \le 172$ in the spanwise (Z) direction. The section of the rigid wall which was replaced with a finite length of the compliant panel from X = 450 – 762 is shown in figure 1. The (X, Y, Z) represents the non-dimensional Cartesian coordinates based on the reference length δ_0 , Where δ_0 = 2.3182 x 10^{-3} m is the displacement thickness at the perturbation location. The number of grid points in X, Y and Z directions are 1200, 85 and 195 respectively. Grid stretching was applied in the y-direction to ensure good and adequate resolution so as to capture fine flow details near the wall. Due to the computational resources limitation, computational domain had to be carefully extended further in order to know where the wavepackets will eventually breakdown into turbulent spots. The initiating pulse (perturbation) was introduced from the wall in a vertical (v-component) direction at the streamwise location X_0 = 349.4 (x_0 = 81cm). The free stream velocity is $U_\infty = 6.65 ms^{-1}$ and the kinematic viscosity is $\upsilon = 1.49 \times 10^{-5} m^2 s^{-1}$, and while the Reynolds number $\mathrm{Re}_\delta = \delta U_\infty / \upsilon$ at the excitation source is 1034.6. The u-velocity component of the disturbance wavepacket were obtained at $y/\delta \approx 0.62$, similar to the heights at which wave measurements were made in the experiments of Cohen et al (1991) and Medeiros & Gaster (1999b). All other imposed simulation conditions and set-ups could be seen in the already published work of Yeo et al (2010).

Figure 1 Schematic plan view showing the location of the compliant panel in the computational domain

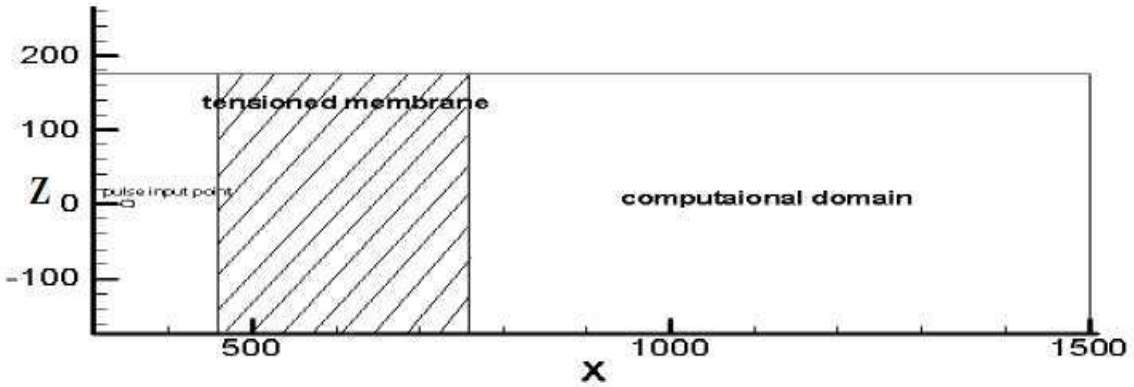

The properties of the membrane panel used are: $m_L = 1.0, T_L = 10.0, d_L = 0.1$ and $k_L = 0$ **Error! Reference source not found.**, based on a wall Reynolds number of $\mathrm{Re}_L = 580$ **Error! Reference source not found.**. A moderately flexible membrane was selected in order to inhibit the compliance-induced flow instabilities (CIFI)/flow-induced surface instabiliti-es (FISI), while yet retaining its capability to stabilize TS waves and hopefully delay transition. A computational simulation is carried out in terms of the global length scale δ_0 **Error! Reference source not found.**. The non-dimensional simulation time **Error! Reference source not found.** $T = tU_\infty / \delta_0$ is estimated from the time of pulse initiation.

2 Results and discussions

Detail numerical study of the continuous transition process of the wavepacket as it travels over the finite length of the compliant panel, from their pulsed inception to their breakdown into the incipient turbulent spots will be presented and discussed in terms of their spatial and spectral aspects of the evolution process. Comparison would be made with the earlier simulation results

obtained for the purely rigid wall case, so as to appreciate the effect of compliant panel in delaying transition further.

2.1 Spatial evolution analysis

The evolution and breakdown of the v-initiated wavepacket is presented in figure 2, where the u-velocity components of the disturbance wavepacket at the height of **Error! Reference source not found.** $y/\delta \approx 0.62$ are shown. At time T = 260, the wavepackets both almost have the same shape and maximum velocity of 0.77% for over the rigid wall case and one with compliant panel case. This shows that the effect of the inserted panel is not yet felt as the wavepacket is just about to climb the compliant panel region. Figure 2(b2) (T = 930) shows the wavepackets are actually travelling on top of the compliant panel. The effect of the compliant panel in suppressing the growth of the wavepacket could be clearly seen at this evolution time, as the wavepacket (triangular) shape in figure 2(b2) grew lesser than its counterpart in Figure 2(b1) which looks crescent-shaped. Though, the wavepackets amplitude in figure 2(b2) is larger than its rigid wall counterparts in figure 2(b1). Down the lane, at time T = 2788, the rigid wall case in figure 2(f1) began to break down into formation of turbulent spots, whereas, over the compliant panel figure 2(f2) still at the earlier part of the nonlinear stage with a maximum u-velocity of 0.74%. In order to see where the wavepacket over the panel case will break down, the computational domain was further extended carefully, keeping the vertical and spanwise size the same. The wavepacket finally break into formation of turbulent spot figure 3(d) with the center location at X = 1970, this translate to a further transition distance of ΔX = 550, when compared with the rigid wall case in the previous study by Yeo et al (2010) that broke down at X = 1420. This translates to approximately 51% increase in the transition distance measured from the point of wavepacket initiation.

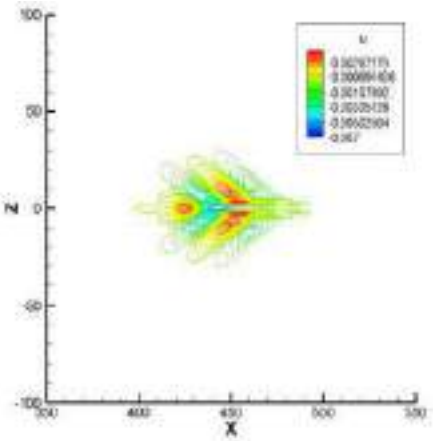

Min: -0.0077 Max: 0.0051

(a1)

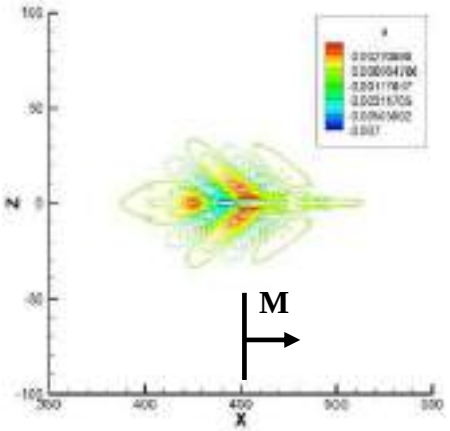

Min: -0.0077 Max: 0.0051

(a2)

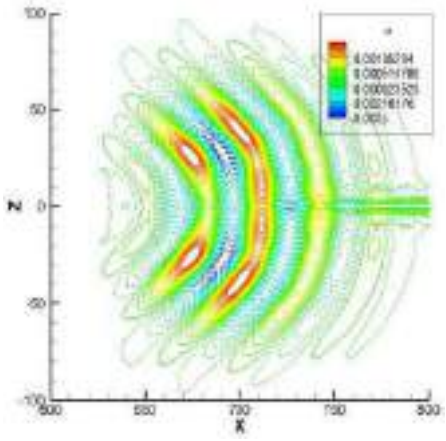

Min: -0.0037 Max: 0.0035

(b1)

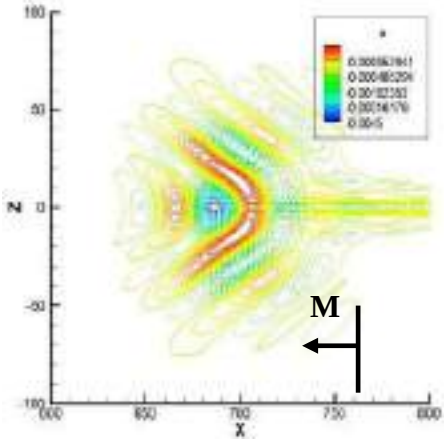

Min: -0.0047 Max: 0.0023

(b2)

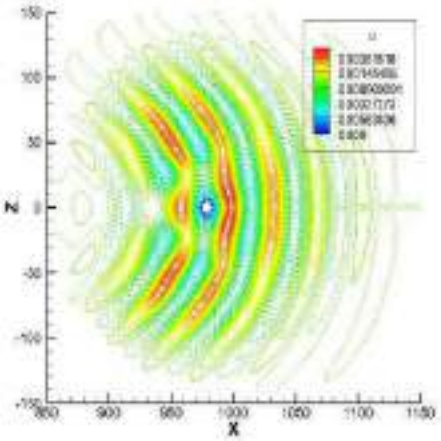

Min: -0.0091 Max: 0.0052

(c1)

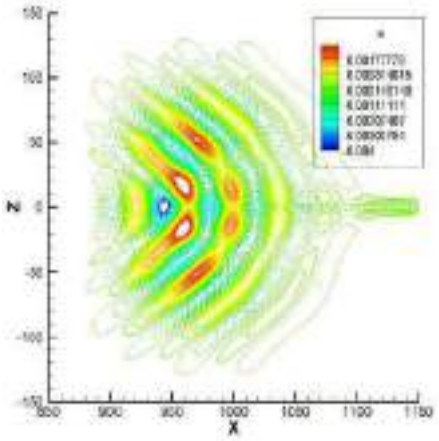

Min: -0.0044 Max: 0.0031

(c2)

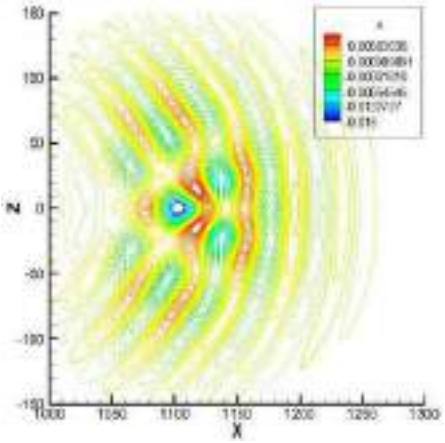

Min: -0.0204 Max: 0.0089

(d1)

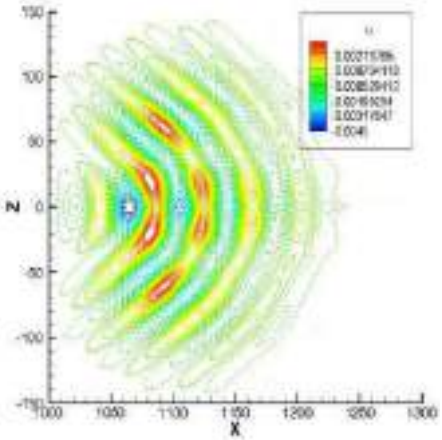

Min: -0.0049 Max: 0.0033

(d2)

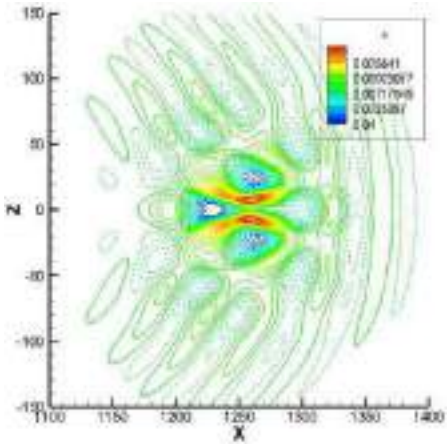

Min: -0.0459 Max: 0.0448

(e1)

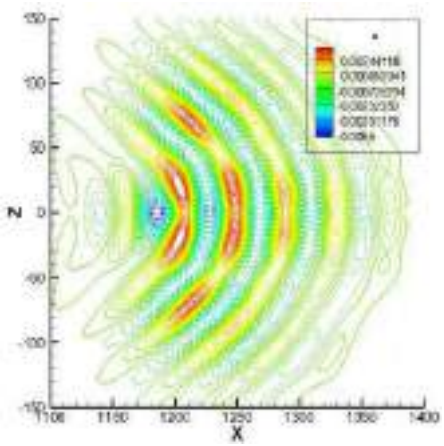

Min: -0.0059 Max: 0.0039

(e2)

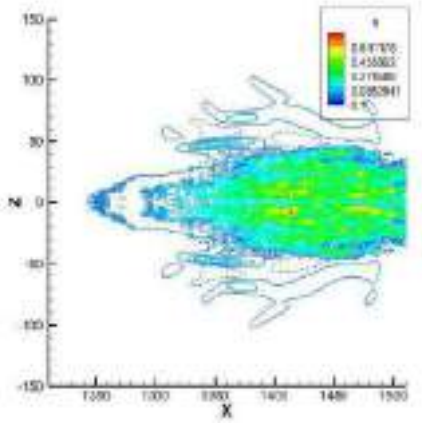

Min: -0.1537 Max: 0.8930

(f1)

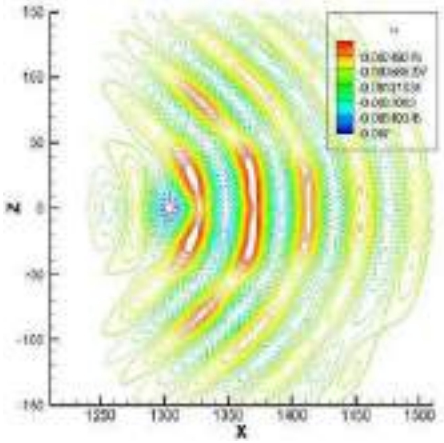

Min: -0.0074 Max: 0.0047

(f2)

Figure 2 Contours of disturbance streamwise velocity u for *v*-initiated wavepacket at y/δ ≈ 0.62**Error! Reference source not found.** times: (a) T = 260; (b) T = 930; (c) T = 1670; (d) T = 2046; (e) T = 2417; (f) T = 2788. Left column for the rigid wall case, while the right column for the compliant panel case. Solid lines represent positive contours and dotted lines represent negative contours. Minimum and Maximum contour values are indicated. M denotes membrane panel boundary location.

Figure 4 shows the compliant panel displacement along the center line (Z = 0). Figure 4(a) shows the displacement of the surface at time T = 186, when the front proper of the wavepacket is still some distance from the leading edge of the panel. The impending arrival of the wavepacket is already felt at the compliant (membrane) surface, which responds with the generation of a fairly regular wave train. This phenomenon of the leading edge (a point of singularity) acting as a source of CIFI waves on a compliant surface when subjected to flow perturbation has been highlighted by Yeo et al. (1999), Wang et al. (2003, 2005) and Wiplier & Ehrenstein (2000,2001). The driven or excited waves are most probably a native CIFI mode of the coupled membrane-flow system. Indeed one may even discern the reflection of the wave from the trailing edge. At time T=260 in figure 4(b), the front of the wavepacket has just arrived at the membrane,

causing a sharp localized increase in the displacement at the front of the membrane.

Localized high-amplitude displacement regions in figures 4(c)-(d) on the membrane surface clearly mark the passage of the wavepacket over the membrane surface. The localized response of the membrane can be more clearly seen in the displacement contours in figures 4(a)-(c), which show the footprints of the wavepacket as it comes onto and travel over the membrane. Figure 4(d) shows the wavepacket as it reaches the end of membrane and the reflection of waves from the trailing edge. The reflection of waves from the trailing edge of the membrane panel can be more clearly seen in the displacement contours over the whole membrane in figure 4(d), which shows inverted crescent-shaped disturbances, as the wavepacket trails out of the membrane panel. The disturbances on the membrane die away gradually when the wavepacket convects further downstream in figures 4(e)-(f). The maximum displacement of the membrane reaches only up to about 0.24% of the local displacement thickness, which shows that the linearization assumption for coupled interaction is justified.

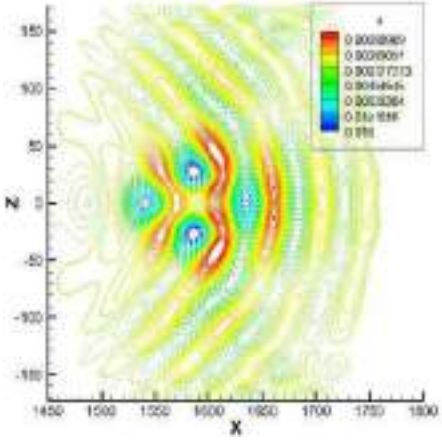

Min: -0.0180 Max: 0.0092

(a)

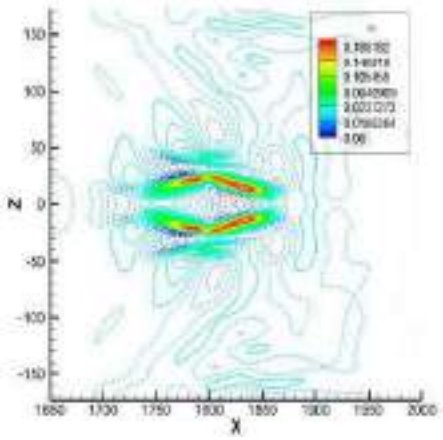

Min: -0.0668 Max: 0.2210

(b)

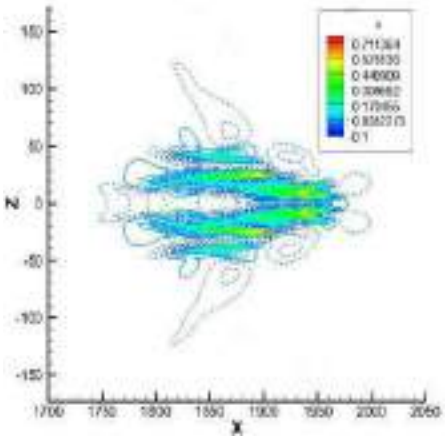

Min: -0.1231 Max: 0.7815

(c)

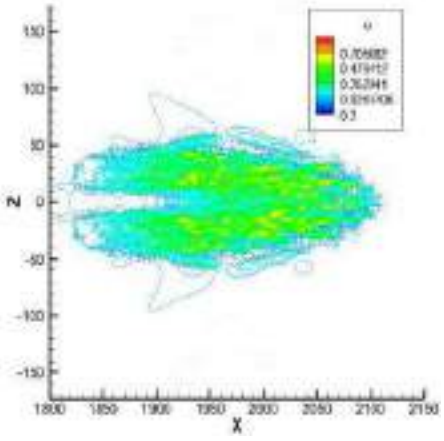

Min: -0.2903 Max: 0.9250

(d)

Figure 3 Contours of disturbance streamwise velocity u for ν-initiated wavepacket at $y/\delta \approx 0.62$ for the one panel membrane case (extended domain) at times: (a) T = 3534; (b) T = 4092; (c) T = 4278; (d) T = 4464. Solid lines represent positive contours and dotted lines represent negative contours. Minimum and Maximum contour values

are indicated.

2.2 Spectral analyses

In order to properly understand the dynamics of wavepackets evolutions, flow quantities were examined further at the height $y/\delta \approx 0.62$ similar to height used by Cohen et al (1991), at different streamwise x-locations by fast Fourier transform (FFT) in time domain and double Fourier transform (DFT) in the space domain. In order to appreciate the function of the inserted finite length of the compliant panel, comparison were made between the earlier obtained simulation results by Yeo et al (2010) for flow over purely rigid wall and for the latest flow over when compliant panel was inserted. Nyquist criterion was duly observed during sampling. Figures 5 and 6 show the frequency-spanwise wavenumber (ω, β) spectral of the disturbance velocity components u (streamwise velocity) and v (wall-normal velocity) respectively. In figure 5(a2), the wavepacket is totally travelling on top of the compliant panel region, and the spectra of the wavepacket at this location shows weak low frequency 2-D (spanwise wavenumber $\beta \approx 0$) waves, which is absent in its counterpart for over the rigid wall spectral in figure 5(a1). These 2-D or nearly 2-D waves present in the wavepacket have something to do with its interaction with the compliant panel, which could be seen or observed in the membrane displacement contours in figure 4.

It was noticed that the said low frequency continue to die away as the wavepacket convects away from the compliant surface region. A conspicuous difference in spectral plot appearance began to be noticed at X = 863 for both over the rigid wall and with the one with compliant surface in figures 5(b1) and 5(b2). At this location X = 863, that is, after the wavepacket had already passed over the compliant surface, the compliant wavepacket in figure (b2) loses most of its higher frequency 2-D waves ($\omega \approx 0.065$) and it is dominated by two oblique wave modes, whereas over the rigid wall own in figure 5(b1), the wavepacket retains a significant content of the 2-D waves. As the wavepacket convects downward further, the dominant 2-D wave modes continue to amplify over the rigid wall case from figure 5(b1) until it reaches a size that allows it to interact effectively with the accompanying oblique wave pair (which have also grown correspondingly) by the nonlinear instability mechanisms of Craik (1971) or Herbert (1988), leading to the accelerated growth of the oblique wave pair in figures 5(c1)-(d1). From there onwards, further strong nonlinear interactions between the dominant oblique wave pair result in the development of low (near-zero) frequency waves for over the rigid wall wavepacket in figures 5(e1) and 6(e1), and the final breakdown of the rigid wall wavepacket in figures 5(f1) and 6(f1). The corresponding comparative spectral dynamics behaviors in the wall normal (v) direction are shown in figure 6.

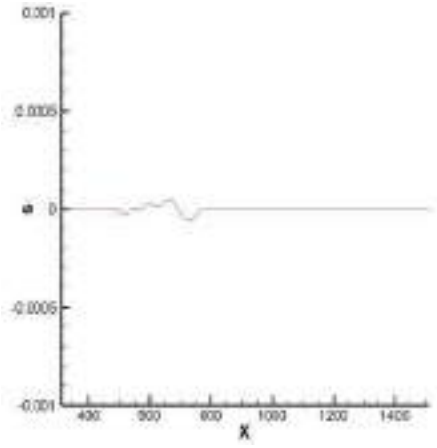

(a)

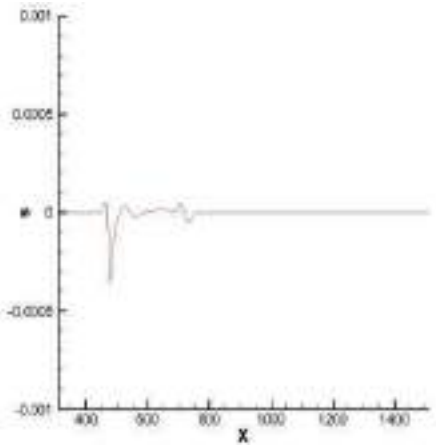

(b)

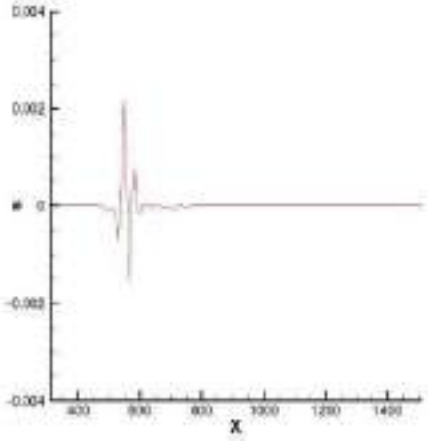

(c)

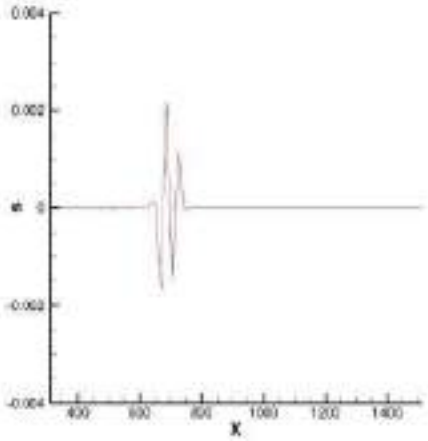

(d)

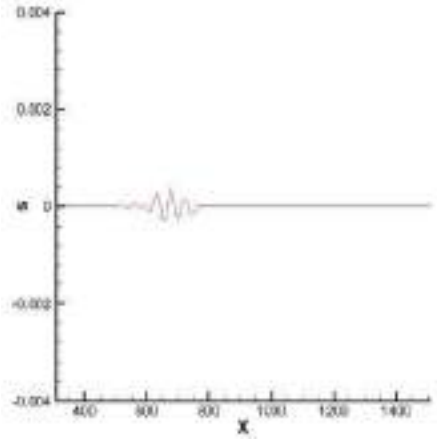

(e)

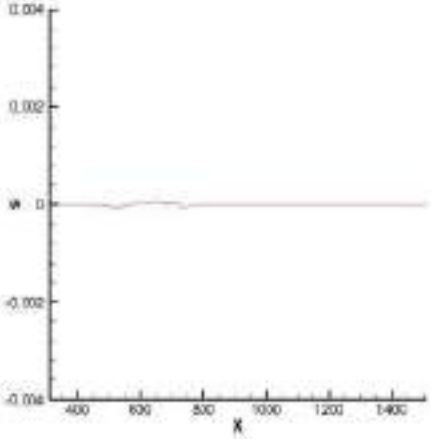

(f)

Figure 4 Membrane displacement evolutions along the centre line for different evolution times. (a) T = 186; (b) T = 260; (c) T = 558; (d) T = 930; (e) T = 1300; (f) T = 1670.

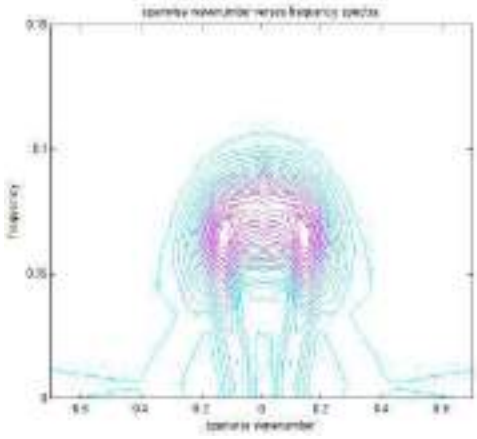

(a1)

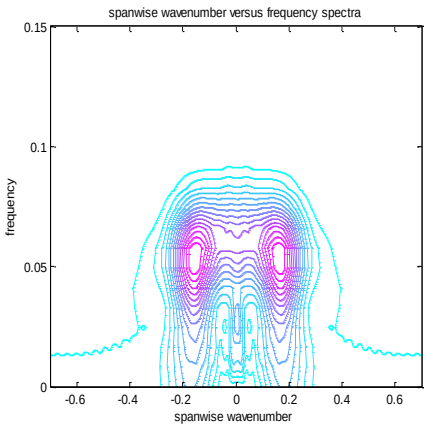

(a2)

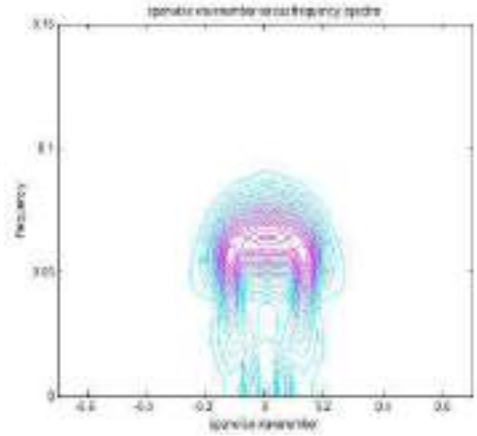

(b1)

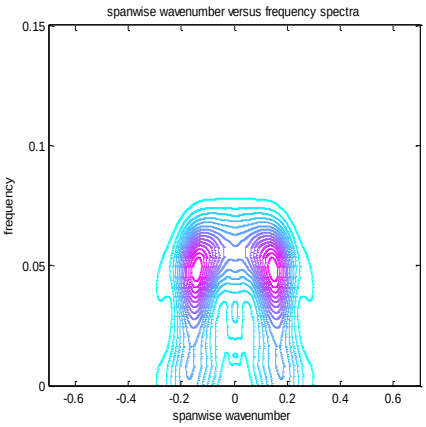

(b2)

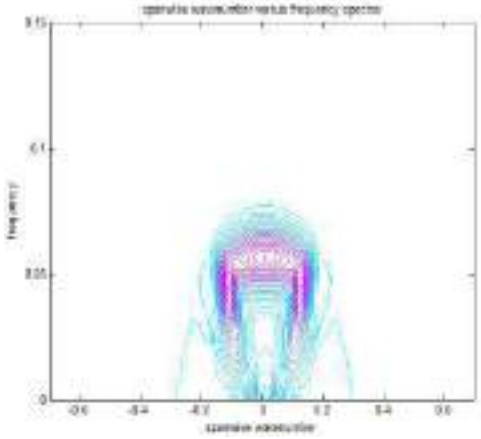

(c1)

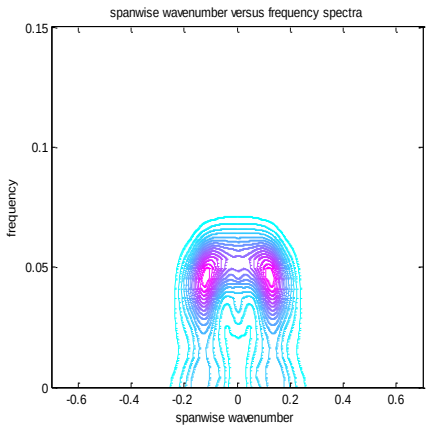

(c2)

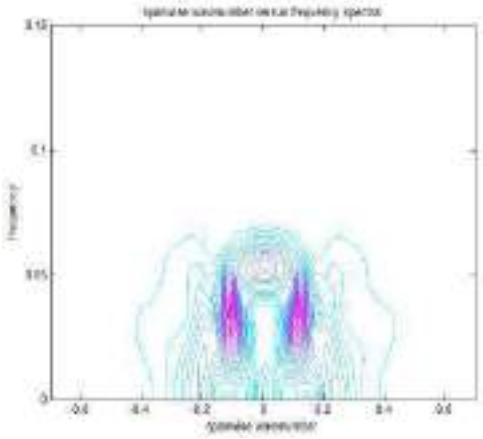

(d1)

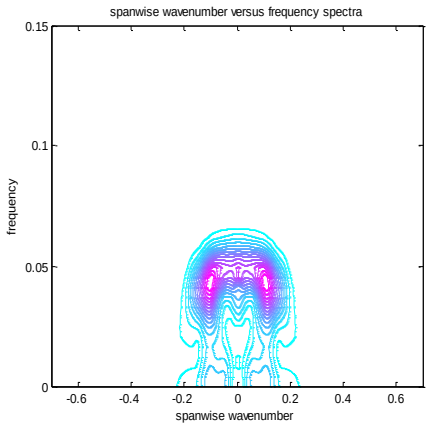

(d2)

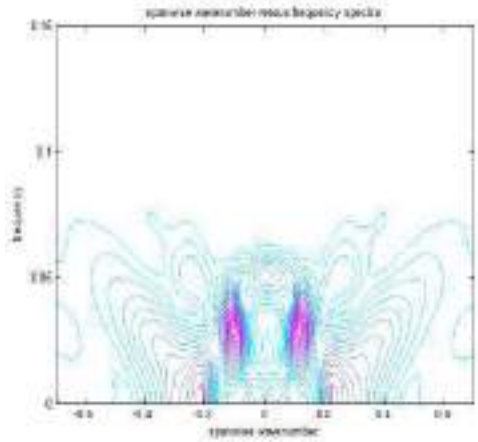

(e1)

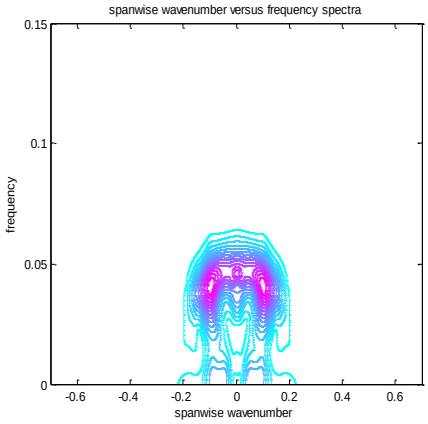

(e2)

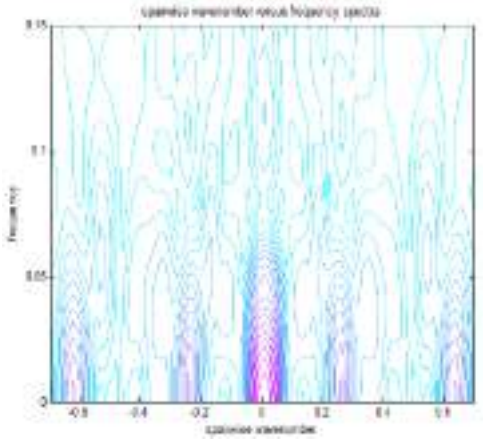

(f1)

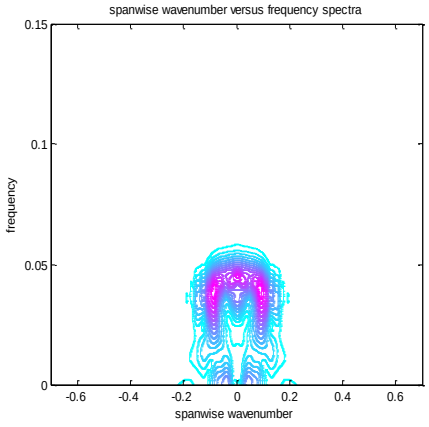

(f2)

Figure 5 Comparison of spanwise wavenumber versus frequency spectra of streamwise u-velocity for different downstream locations at y/δ ≈ 0.62 between rigid wall case (left column) and with compliant panel case (right column); δ denotes the local displacement thickness. (a) X=690; (b) X=863; (c) X=1035; (d) X=1208; (e) X=1294; (f) X=1467.

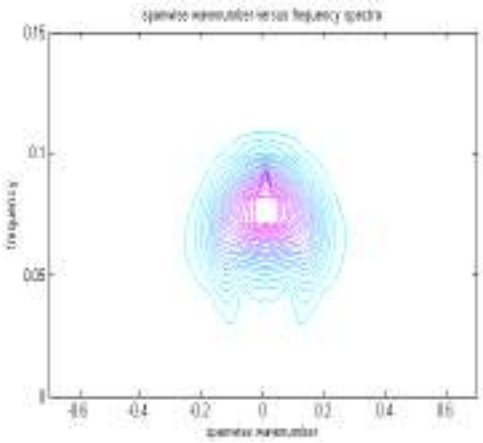

(a1)

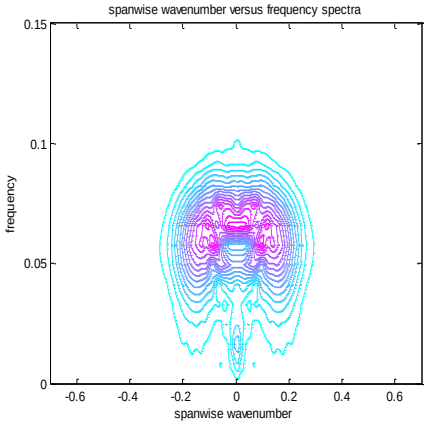

(a2)

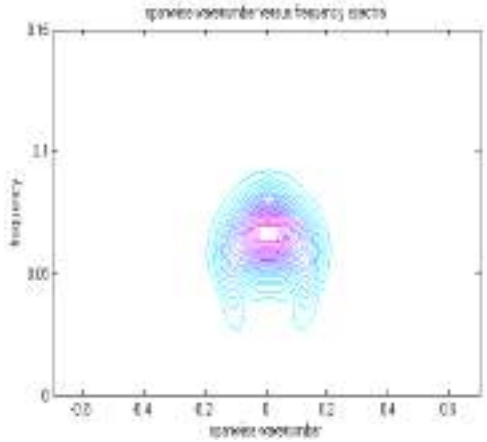

(b1)

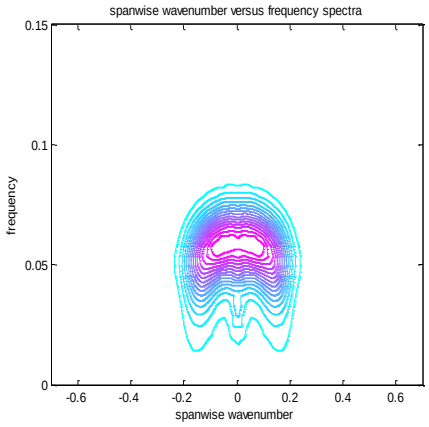

(b2)

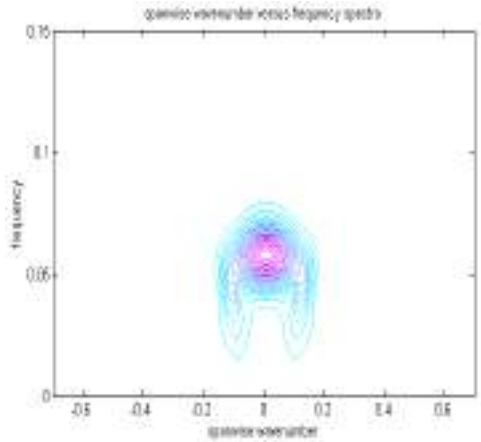

(c1)

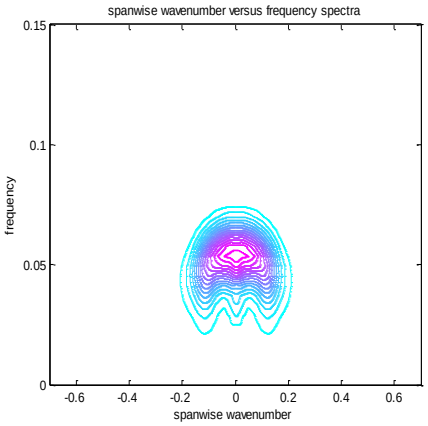

(c2)

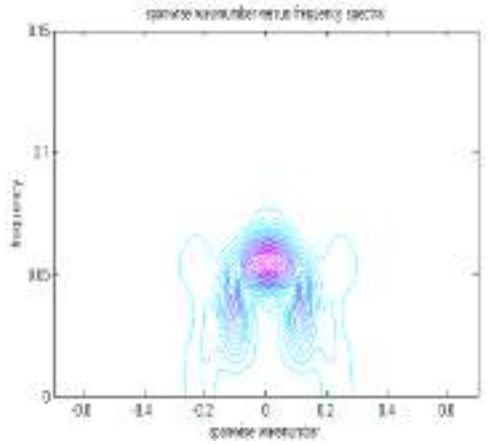

(d1)

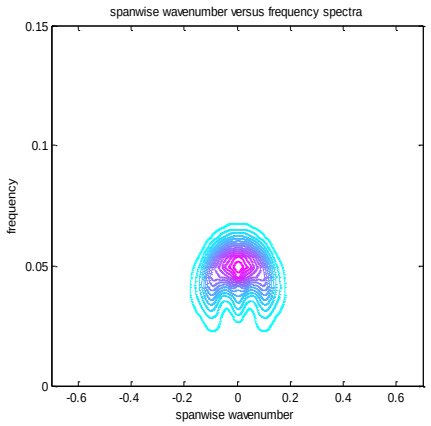

(d2)

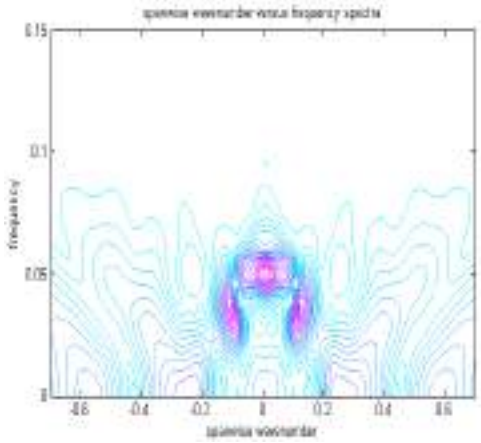

(e1)

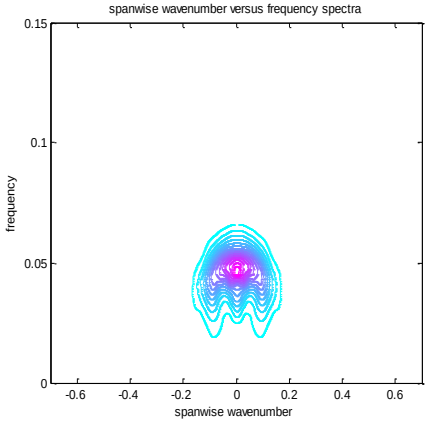

(e2)

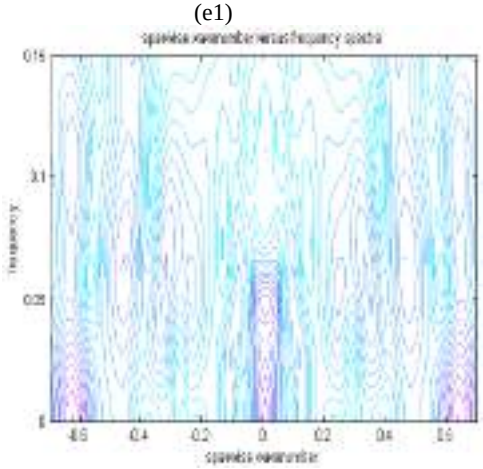

(f1)

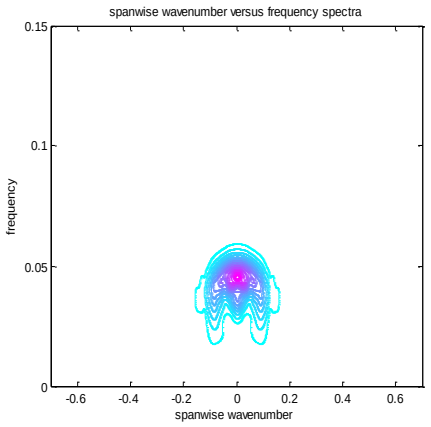

(f2)

Figure 6 Comparison of spanwise wavenumber versus frequency spectra of wall-normal v-velocity for different downstream locations at y/δ ≈ 0.62 between rigid wall case (left column) and with compliant panel case (right column); δ denotes the local displacement thickness. (a) X=690; (b) X=863; (c) X=1035; (d) X=1208; (e) X=1294; (f) X=1467.

3 Conclusions

Investigations on the use of a short compliant panel to delay transition further within a Blasius boundary layer through DNS had been reported. Small section of the rigid wall was replaced with a finite compliant length from X = 450 – 762, and perturbation was carried out via introduction of vertical component (v) velocity pulse at the flow upstream, that is, before the compliant panel location. A flexible compliant panel was carefully chosen with the aim to be able to stabilize TS waves and same time help in delaying transition further. Also, compliant panel length has been selected to be short enough so as to discourage the formation of static divergence (SD) waves and inhibit the propagation of the travelling wave flutter (TWF) waves using a modified potential analysis. From the spatial evolution results for the computational domain with inserted compliant panel, breakdown into formation of turbulent spots occurred with center location at X = 1970, and whereas for the earlier published rigid wall case (that is, no compliant panel inserted), formation of turbulent spots occurred at X = 1420. By comparing these two cases, this translates to approximately 51% increase in the transition distance measured from the point of wavepacket initiation, when a short complaint panel was used.

In addition, spectrum analysis results show that the interaction of the compliant panel with the wavepacket when evolving over it caused suppression of 2-D wave mode. This confirms that the compliant panel is able to effectively attenuate the linearly growing primary 2-D TS wave mode, so that resultant wavepacket after the membrane panel was dominated by a pair of oblique waves. The present study shows that attenuating the growth of the linearly evolving TS waves at its early stages and extending the linear regime correspondingly presents an effective strategy to delay transition. With this study, it shows that proper incorporation of compliant panel in the real life designs and applications will be one of the promising means for drag reductions in time to come.

References

1 Blick E.F. & Walters R.R., 1968, Turbulent boundary layer characteristics of compliant surfaces, J. Aircr. 5(1) p. 11-16

2 Bushnell D.M., Hefner J.N. & Ash R.L., 1977, Effect of compliant wall motion on turbulent boundary layer, Phys. Fluids 20 (10), p. 31-48

3 Chu H.H. & Blick E.F., 1969, Compliant surface drag as a function of speed, J. Spacecr. Rockets 6(6), p. 763-764

4 Cohen J., Breuer K. S. & Haritonidis J. H., 1991, On the evolution of a wave packet in a laminar boundary layer, J. Fluid Mech. 225, p. 575-606

5 Colley A. J., Thomas P. J., Carpenter P.W., & Cooper A.J., 1999, An experimental study of boundary layer transition over a rotating, complaint disk. Phys. Fluids, 11, p. 3340-3352

6 Craik A.D. D., 1971, Nonlinear resonant instability in boundary layers, J. Fluid Mech. 50, p. 393-413

7 Davies C. & Carpenter P. W., 1997, Numerical simulation of the evolution of Tollmien-Schlichting waves over finite compliant panels, J. Fluid Mech. 335, p. 361-392

8 Davies C., 2005, Numerical simulation of boundary-layer disturbance evolution, Phil. Trans. R. Soc. A, 363, 1109 - 1118

9 Domaradzki J.A. & Metcalfe R.W., 1987, Stabilization of laminar boundary layers by compliant membranes, Physics of Fluids, vol.30 (3), p.695

10 Fisher D.H. & Blick E.F., 1966, Turbulent damping by flabby skins, J. Aircr. 3(2), p.163-164

11 Gaster M., 1987, Is the Dolphin a Red Herring?, Turbulence Management and Relaminarisation IUTAM Symposium Bangalore. India. Edited by Liepmann H.W & Narasimha R., p. 285-304

12 Hall M.S., 1988, The interaction between a compliant material and an unstable boundary layer flow, Journal of Computational Physics, vol.76, p.33

13 Herbert T., 1988, Secondary instability of boundary layers, Ann. Rev. Fluid Mech.20, p.487-526

14 Huang J.C, & Johnson M.W., 2007, The influence of complaint surfaces on bypass transition, Exp. Fluids, 42, pp. 711 - 718

15 Kramer M.O., 1957, Boundary layer stabilization by distributed damping, J. Aeronaut. Sci. 24(6), p. 459-460

16 Kramer M.O., 1960, The dolphins' secret. New Scientist 7, 1118-1120

17 Lee T., Fisher M. & Schwarz W.H., 1995, Investigation of the effects of a compliant surface on boundary-layer stability, J. Fluid Mech. 288, p. 37-58

18 Medeiros M.A.F & Gaster M., 1999b, The production of subharmonic waves in the nonlinear evolution of wavepackets in boundary layers, J. Fluid Mech. 399, p. 301-318
19 Metcalfe R.W., Battistoni F., Orzo S. & Ekeroot J., 1991, Evolution of boundary layer flow over a compliant wall during transition to turbulence, Proceedings of Royal Aeronautical Society, p.36.1
20 Nisewanger C.R. 1964, Flow noise drag measurements of vehicle with compliant coatings, US Naval ordnance Test Station Report No.8518
21 Puryear F.W., 1962, Boundary layer control: Drag reduction by use of compliant coatings, Davis Taylor Model Basin Report No.1668
22 Ritter H. & Porteous J.S., 1965, Water tunnel measurements of skin friction on a compliant coating, British Admiralty Research Laboratory Report ARL/N3/G/HY/9/7
23 Wang Z., 2003, Computational simulation of unsteady boundary layer over compliant surfaces, Ph.D. Thesis, National University of Singapore
24 Wang Z., Yeo K.S. & Khoo B.C., 2001, Numerical simulation of 2D Tollmien-Schlichting waves over finite membrane, Proceedings of 9th Annual Conference of the CFD Society of Canada, p453
25 Wang Z., Yeo K.S., Khoo B.C., 2005, On two-dimensional linear waves in Blasius boundary layer over viscoelastic layers, European Journal of Mechanics B/Fluids 25, p.33-58
26 Willis G .J. K., 1986, Hydrodynamic stability of boundary layers over compliant surfaces, PhD Thesis, Cambridge University, U.K, p. 243
27 Wiplier O. & Ehrenstein U., 2000, Numerical simulation of linear and nonlinear disturbance evolution in a boundary layer with compliant walls, Journal of Fluids and Structures 14, p.157-182
28 Wiplier O. & Ehrenstein U., 2001, On the absolute instability in a boundary-layer flow with compliant coatings, European Journal of Mechanics. B-Fluids, vol.20, p. 127
29 Yeo K.S. 2010, DNS of wavepacket evolution in a Blasius boundary layer. Journal of fluid mechanics, vol. 652, pp. 333-372
30 Yeo K.S., Khoo B.C. & Zhao H.Z., 1999, The convective and absolute instability of fluid flow over viscoelastic compliant layers, Journal of Sound and Vibration.223(3), p.379-398
31 Zhao X., 2006, Computational simulation of wavepacket evolution over complaint surfaces, Ph.D. Thesis, National University of Singapore